Analysis of Channel-Averaged SINR for Indoor UWB Rake and Transmitted Reference Systems

Tao Jia, *Student Member, IEEE*, and Dong In Kim, *Senior Member, IEEE*

***Abstract*—In this paper, we derive a closed-form expression for *channel-averaged* signal-to-interference-plus-noise ratio (SINR) for ultra-wideband (UWB) Rake receiving system in an indoor multiuser communication scenario, given that the interference level is fluctuating due to asynchronous transmissions among users. The indoor wireless channel model adopted here is a standard one, recently released by IEEE 802.15 study group 3a [1]. We propose a theoretical framework to derive the channel-averaged SINR considering the lognormal channel gain distribution and the double independent Poisson arrival distribution of cluster and ray, and show that our analysis is well coincident with the simulation results. With this framework, we demonstrate that our analysis can be applied to theoretically determine the optimum integration interval for a UWB transmitted reference system, even in a multiuser scenario.**

***Index Terms*—Channel-averaged signal-to-interference-plus-noise ratio (SINR), double Poisson process, lognormal distribution, Rake receiver, transmitted reference (TR) system, ultra-wideband (UWB).**

I. Introduction

ULTRA-WIDEBAND (UWB) technology has been proposed as a promising alternative for indoor wireless communication systems to support short-range high-data rate transmissions. The carrierless transmitted signal is composed of a sequence of low-duty-cycle subnanosecond pulses. The high ratio of the transmitted signal bandwidth to the information rate provides UWB system with multiple-access capability. In [2] and [3], the authors proposed time-hopping (TH) impulse radio as the multiple-access scheme and analyzed the performance of a TH pulse position modulation (TH-PPM) UWB system based on the Gaussian approximation of multiple-access interference (MAI). In TH-UWB system, each symbol period is divided into a number of frames and only one pulse is transmitted in each frame. The position of the pulse within each frame is determined by a user-specific pseudorandom sequence to avoid *catastrophic collision* among different users. In [4], the authors derived an exact BER expression using the characteristic function method and evaluated the accuracy of Gaussian approximation used in [2] and [3]. However, all these papers examined only the system performance based on additive white Gaussian noise (AWGN) channel.

The bandwidth occupancy of UWB signal from near dc to a few gigahertz leads to fine multipath resolvability, which significantly reduces fading effects in indoor environments [5]. In [6], the authors provided experimental results for the performance of UWB Rake receiver in a dense multipath environment. To precisely analyze the performance of a UWB system, great efforts have been made on developing an appropriate channel model to capture the characteristics of UWB signal. Recently, IEEE 802.15 study group 3a has accepted the indoor wireless channel model developed at Intel for high-data rate UWB systems [1], in which the clustering of path arrivals was reported. Specifically, the multipath components arrive according to a double Poisson process and the fading coefficient of each multipath component has an independent lognormal distribution rather than Rayleigh distribution. Furthermore, the double-exponential model was found to be better fit for the power decay profile. Based on this channel model, [7]–[9] presented signal-to-noise ratio (SNR) and bit-error-rate (BER) performance for different types of Rake receivers. However, they only considered single-user transmission. Besides, the results are given in a semianalytical way.

Due to the large number of multipath components, Rake receiver may not be suitable for collecting enough signal energy with only moderate receiver complexity [5]. Moreover, the imperfect channel estimation may affect the system performance severely. Alternatively, the authors in [10] proposed UWB transmitted reference (UWB-TR) system, in which the receiver correlates the received data signal with the unmodulated reference signal and integrates over a certain time interval to collect enough signal energy. UWB-TR signaling accomplishes channel estimation and collects the desired signal energy in such a simple way at the expense of increased noise power, due to noise-times-noise operation. In [11], the authors found the optimum integration interval by maximizing the average output SNR for a single-user UWB-TR system. [12] and [13] also used the optimized integration interval when analyzing UWB-TR sytem performance. However, in all these papers, the optimum integration interval is determined through simulations for a single-user link, given a certain input SNR. The optimized integration interval may not be optimum for higher (lower) input SNR values, since we have more (less) reliable multipath components that can be included for detecting the data

Paper approved by S. N. Batalama, the Editor for Spread Spectrum and Estimation of the IEEE Communications Society. Manuscript received May 17, 2005; revised August 28, 2006. This work was supported by the Ministry of Information and Communication (MIC), Korea, under the Information Technology Research Center (ITRC) Support Program supervised by the Institute of Information Technology Assessment (IITA). This paper was presented in part at the IEEE VTC Spring '05 Conference, Stockholm, Sweden, May 2005.

T. Jia is with the Bradley Department of Electrical and Computer Engineering, Virginia Polytechnic Institute and State University, Blacksburg, VA 24060 USA (e-mail: taojia@vt.edu).

D. I. Kim was with the School of Engineering Science, Simon Fraser University, Burnaby, BC V5A 1S6, Canada. He is now with the School of Information and Communication Engineering, Sungkyunkwan University, Suwon 440-746, Korea (e-mail: dikim@ece.skku.ac.kr).

Digital Object Identifier 10.1109/TCOMM.2007.906435

bit. Similarly, the optimum integration interval determined for a single-user link may no longer be optimum as far as the MAI is concerned.

In this paper, we begin with analyzing the performance of Rake receiving system, such as partial Rake (*p-Rake*), in terms of *channel-averaged* output SINR in typical indoor multiuser environments. To this end, we propose a theoretical framework to derive a closed-form expression for channel-averaged output SINR based on the IEEE 802.15.3a channel model and show that our analysis is well coincident with the simulation results. Based on this framework, we can compare the performance of UWB Rake receiving system in different types of indoor wireless channels, using the channel-averaged SINR as a performance measure. We further attempt to derive a closed-form expression for BER based on our model. However, to the best of the authors' efforts, we find that without much affecting the essence of the channel characteristics, the derivation of a closed-form BER expression is unwieldy.

Another application of the theoretical framework, developed in this paper, is to determine the optimum integration interval for a single-user UWB-TR system by maximizing the channel-averaged output SNR. We compare the analytical optimum integration interval with the one determined by minimizing average BER obtained through simulation, and show that there is little difference between them for low and medium SNRs. We also demonstrate that, depending upon the input SNR, the optimum integration interval will be different and there exists a lower bound on the integration interval, corresponding to extremely low input SNR. Our results reveal that, using the lower bound as the integration interval for all input SNRs will cause some performance degradation, especially for high input SNR. Finally, we extend the analysis to the multiuser scenario and show that as far as the MAI is concerned, the optimum integration interval will decrease as the number of users increases. We also find that in the multiuser scenario, using the lower bound as the integration interval is a good choice to somehow reduce the receiver complexity without causing too much performance loss.

The rest of the paper is organized as follows. Section II describes the signaling format for a TH-pulse position modulation (PPM) UWB system along with the channel model. Section III specifies the receiver structure and mathematical model used to analyze the channel-averaged output SINR for a *p*-Rake receiver. Section IV gives the signal model for UWB-TR system and elaborates how to use our theoretical framework to determine the optimum integration interval. Numerical and simulation results are presented in Section V and concluding remarks are given in Section VI.

II. Signal and Channel Models

We consider TH-binary PPM (BPPM) as the signaling format. The transmissions from different users are assumed to be asynchronous. Each user is assigned a random TH pattern to avoid catastrophic collision with others. The TH-BPPM signal from νth user is expressed by [3]

$$s^{(\nu)}(t) = \sum_{j=-\infty}^{+\infty} \sqrt{E_w}\, w_{tr}\left(t - jT_f - c_j^{(\nu)} T_c - \delta\, b^{(\nu)}_{\lfloor j/N_s \rfloor}\right) \tag{1}$$

where $w_{tr}(t)$ is a unit-energy transmitted pulse and E_w is the transmitted pulse energy. δ represents the time shift associated with BPPM, and $b^{(\nu)}_{\lfloor j/N_s \rfloor} \in \{0, 1\}$ is the user-specific data sequence ($\lfloor x \rfloor$ denotes the integer part of x). T_f is the frame time in which only one pulse is transmitted and N_s denotes the number of frames per symbol. $c_j^{(\nu)}$ is the TH value for the jth frame of νth user and T_c is the chip duration.

The discrete-time impulse response of the UWB channel model can be written as [1]

$$h(t) = \sum_{l=0}^{L} \sum_{k=0}^{K} \alpha_{k,l}\, \delta(t - T_l - \tau_{k,l}) \tag{2}$$

where $\alpha_{k,l}$ is the gain coefficient of kth ray in lth cluster and $\tau_{k,l}$ is the arrival time of kth ray relative to lth cluster's arrival time T_l. The intercluster and interray arrival times are independently exponentially distributed $\alpha_{k,l} = p_{k,l}\beta_{k,l}$ where $p_{k,l}$ equiprobably takes on the values of ± 1 accounting for the random pulse inversion that occurs due to reflections and $\beta_{k,l}$ is a lognormal random variable, denoted by $20\log_{10}(\beta_{k,l}) \propto N(\mu_{k,l}, \sigma^2)$. The power profile is double exponentially decaying, given by $\boldsymbol{E}\{\beta_{k,l}^2\} = \Omega_0 \exp(-T_l/\Gamma)\exp(-\tau_{k,l}/\gamma)$ ($\boldsymbol{E}$ denotes the expectation), where Ω_0 is the mean power of the first ray of the first cluster, Γ and γ represent the power decay factors of the cluster and ray, respectively.

The signal received by the *desired* first user within one-symbol duration can be written as (assuming symbol '0' was transmitted by the first user)

$$r(t) = \sum_{j=0}^{N_s-1} \sqrt{E_w}\, g^{(1)}\left(t - jT_f - c_j^{(1)} T_c\right) + \sum_{\nu=2}^{N_u} \sum_{j=-\infty}^{+\infty} \times \sqrt{E_w}\, g^{(\nu)}\left(t - jT_f - c_j^{(\nu)} T_c - \delta d^{(\nu)}_{\lfloor j/N_s \rfloor} - \tau_0^{(\nu)}\right) \tag{3}$$

where $g^{(\nu)}(t) = w_{\text{rec}}(t) \otimes h^{(\nu)}(t), \nu = 1, 2, \ldots, N_u$ and N_u is the total number of users. $w_{\text{rec}}(t)$ represents the received pulse, which is usually the time derivative of the transmitted pulse. $h^{(\nu)}(t)$ denotes the channel-impulse response for νth user and is considered to be time-invariant within one symbol duration ($\otimes$ denotes convolution). $\tau_0^{(\nu)}$ represents the νth user's reference delay relative to the first user caused by asynchronous transmission. Without loss of generality, we assume $\tau_0^{(1)} = 0$. $n(t)$ is AWGN with two-sided power spectral density of $N_o/2$.

III. Rake Performance Analysis

To analyze the performance of a practical Rake receiving system, we usually need to make the assumption that the multipath components are isolated and resolvable at the receiver. Based on this assumption, we consider an equivalent discrete-time channel model for (2). Specifically, the whole arrival time

axis is divided into time bins of $\Delta\tau$, which is at least equal to the pulsewidth [6, eq. (5)]. In any given time bin, one or more multipath components (MPCs) can arrive because of *cluster overlapping*, or no arrival at all. The channel gain coefficients of all the arrived MPCs within that time bin are added together to yield a combined channel coefficient. Based on this model, the νth user's equivalent discrete-time channel impulse response can be written as

$$h^{(\nu)}(t) = \sum_i A_i^{(\nu)} \delta(t - \tau_i) \tag{4}$$

where $\tau_i = (i-1)\Delta\tau$ is the ith time bin and $A_i^{(\nu)}$ represents the sum of the channel coefficients of all MPCs arrived in ith time bin. In general, the channel coefficients $\{A_i^{(\nu)}\}$ are correlated for the earlier $\Delta\tau$ (or T_c)-spaced multipath channel model [14], but with $\Delta\tau \ll$ delay spread they can be well approximated to be uncorrelated. Compared with (2), this discrete-time channel model does not account for pulse distortion due to partial *pulse overlapping*, which is very usual when using a large pulsewidth (e.g., 0.7 ns in [12]). However, when considering very small pulsewidth (e.g., 0.167 ns in [1]), the probability of pulse distortion will be greatly reduced. With this small pulsewidth, the equivalent sampling frequency for the discrete-time channel impulse response will be about 6 GHz and (4) will be a good approximation to (2) in terms of preserving most of the channel characteristics.

Based on this discrete-time channel model, a tapped-delay-line Rake receiver structure can be adopted to collect the signal energy in each time bin. For the first user, assuming perfect timing synchronization, the output of the ith Rake finger can be written as

$$Z_i = \sum_{j=0}^{N_s-1} \int_{\tau_i + jT_f}^{\tau_i + (j+1)T_f} r(t) v\left(t - jT_f - c_j^{(1)} T_c - \tau_i\right) dt \tag{5}$$

where $v(t) = w_{\text{rec}}(t) - w_{\text{rec}}(t-\delta)$ is the template signal. Given perfect channel estimation, the decision statistic after maximal-ratio combining (MRC) of the first L_p fingers is expressed by

$$Z = \sum_{i=1}^{L_p} \sqrt{E_w}\, A_i^{(1)} Z_i \tag{6}$$

where $A_i^{(1)}$ represents the channel coefficient of ith time bin of the first user and is assumed to be known at the receiver. To avoid interframe interference (IFI), we assume [3, eq. (57)]

$$N_h T_c + T_m + T_w + \delta \le \frac{T_f}{2} \tag{7}$$

where $N_h T_c$ corresponds to the maximum TH shift, T_m is the channel delay spread, and T_w is the pulsewidth. Based on (7), the *instantaneous* output SINR conditioned on all the channel coefficients of all users can be formulated as

$$\text{SINR}\left(\{A^{(\nu)}\}\right) = \frac{\xi^2}{\sigma_{\text{rec}}^2 + E_w^2 N_s T_f^{-1} \sum_{\nu=2}^{N_u} {G_{\text{eff}}^{(\nu)}}^2} \tag{8}$$

where $A^{(\nu)} = \{A_i^{(\nu)}\}$, and the quantities ξ, σ_{rec}^2, and ${G_{\text{eff}}^{(\nu)}}^2$, which represent desired signal, filtered noise, and MAI, respectively, can be evaluated in a similar way as [3], denoted by

$$\xi = E_w N_s R(0) \sum_{i=1}^{L_p} {A_i^{(1)}}^2 \tag{9}$$

$$\sigma_{\text{rec}}^2 = N_o E_w N_s R(0) \sum_{i=1}^{L_p} {A_i^{(1)}}^2 \tag{10}$$

$${G_{\text{eff}}^{(\nu)}}^2 = \sum_{i,\,k=1}^{L_p} \sum_{n,\,m=1}^{N} A_i^{(1)} A_k^{(1)} A_n^{(\nu)} A_m^{(\nu)} Q[(i-k-n+m)\Delta\tau] \tag{11}$$

where the conditional expectation on MAI does not depend on TH sequences as long as (7) is valid, $R(\cdot)$ represents the correlation function between the received pulse $w_{\text{rec}}(t)$ and template signal $v(t)$. N is the total number of time bins to be considered for each channel realization and $Q(\cdot)$ is defined as the autocorrelation function of $R(\cdot)$, i.e., $Q(x) = \int_{-\infty}^{+\infty} R(\tau) R(\tau + x) d\tau$.

To find the *channel-averaged* SINR, which is defined by

$$\begin{aligned}\text{SINR} &\triangleq \overline{\text{SINR}(\{A^{(\nu)}\})} \\ &= \frac{|\boldsymbol{E}_{A^{(1)}}\{\xi\}|^2}{\boldsymbol{E}_{A^{(1)}}\left\{\sigma_{\text{rec}}^2 + E_w^2 N_s T_f^{-1} \sum_{\nu=2}^{N_u} \boldsymbol{E}_{A^{(\nu)}}\left\{{G_{\text{eff}}^{(\nu)}}^2 | A^{(1)}\right\}\right\}},\end{aligned} \tag{12}$$

we need to take another expectation with respect to the channel realization. Here, the first-order approximation[1] is made to the desired signal ξ as its mean $\boldsymbol{E}_{A^{(1)}}\{\xi\}$, while the MAI is accounted for in terms of the second-order moment due to *time asynchronism*, given the channel coefficients of the *desired* first user that are being *estimated*. Considering the interference part (i.e., MAI), we need to evaluate $\boldsymbol{E}_{A^{(\nu)}}\{{G_{\text{eff}}^{(\nu)}}^2 | A^{(1)}\}$. For a specific channel realization, we have $A_n^{(\nu)} = \sum_q p_{n,q}^{(\nu)} \beta_{n,q}^{(\nu)}$ and $A_m^{(\nu)} = \sum_u p_{m,u}^{(\nu)} \beta_{m,u}^{(\nu)}$, where $(p_{n,q}^{(\nu)},\, p_{m,u}^{(\nu)})$ equiprobably take on the values of ± 1 and $(\beta_{n,q}^{(\nu)},\, \beta_{m,u}^{(\nu)})$ represent the qth and the uth MPCs arrived in the nth and the mth time bins, respectively. Note that there is some difference between the definition for the subscripts of $\beta_{n,q}^{(\nu)}$ and that of $\beta_{k,l}$ in (2), because the former accounts for any possible overlapping among MPCs based on our discrete-time channel model. Due to the independency between different MPCs and the fact that $\boldsymbol{E}\{p_{n,q}^{(\nu)}\} = 0$ and $\boldsymbol{E}\{{p_{n,q}^{(\nu)}}^2\} = 1$, we have

$$\boldsymbol{E}\left\{A_n^{(\nu)} A_m^{(\nu)}\right\} = \begin{cases} \boldsymbol{E}\left\{{A_n^{(\nu)}}^2\right\} = \sum_q \boldsymbol{E}\left\{{\beta_{n,q}^{(\nu)}}^2\right\}, & n = m \\ 0, & n \ne m. \end{cases} \tag{13}$$

[1]The first-order SINR approximation is validated through the BER simulations in Fig. 7, where the two methods have been compared in determining the optimum integration interval for TR systems.

Using this result, the conditional expectation of (11) will have nonzero components only when $n = m$. Furthermore, due to zero-crossing property of $R(\cdot)$ and the limited supporting range of $Q(\cdot)$, we have $Q(\pm\Delta\tau) \ll Q(0)$ and $Q[(i-k)\Delta\tau] = 0$ when $|i-k| \geq 2$. Consequently, only the terms corresponding to $i = k$ and $n = m$ will be left, resulting in

$$\boldsymbol{E}_{A^{(\nu)}}\left\{{G_{\text{eff}}^{(\nu)}}^2 | A^{(1)}\right\} = Q(0)\sum_{i=1}^{L_p}{A_i^{(1)}}^2 \sum_{n=1}^{N}\boldsymbol{E}\left\{{A_n^{(\nu)}}^2\right\}. \tag{14}$$

Substituting (14) into (12), the channel-averaged SINR can be formulated as

$$\text{SINR} = \frac{E_w N_s R^2(0)\sum_{i=1}^{L_p}\boldsymbol{E}\left\{{A_i^{(1)}}^2\right\}}{N_o R(0) + E_w Q(0) T_f^{-1}\sum_{\nu=2}^{N_u}\sum_{n=1}^{N}\boldsymbol{E}\left\{{A_n^{(\nu)}}^2\right\}}. \tag{15}$$

The computation of (15) requires the evaluation of average path energy. Recalling our discrete-time channel model, there could be MPC arrival or not in any given time bin. In the following, when we mention a *cluster arrival* in any given time bin, we refer to the arrival of the first ray component within this cluster. Accordingly, a *ray arrival* is always referring to the arrival of a ray component other than the first one within each cluster.

With the very small $\Delta\tau$ in our assumption, it is well known that Poisson arrival process can be approximated by binomial distribution.[2] Specifically, there could be one or no cluster arrival in $\Delta\tau$ with the probabilities given by $P_c \triangleq \Lambda\Delta\tau$ and $1 - P_c$, respectively. In addition, given a cluster arrival in a certain time bin, there could be one or no ray arrival in any following time bin with the probabilities given by $P_r \triangleq \lambda\Delta\tau$ and $1 - P_r$, respectively (Λ and λ are defined as the cluster and ray arrival rates, respectively). The probability that there are more than one cluster arrival in any time bin is zero. Similarly, within the same cluster, the probability that there are more than one ray arrival in any time bin is also zero. Based on this assumption, there are only a *finite number* of arrival patterns in each time bin and the average path energy can be evaluated in a unified way no matter which channel model has been chosen, i.e., line-of-sight (LOS) or nonline-of-sight (NLOS).

In the evaluation of average path energy, we find the following lemma useful.

Lemma: The probability that qth $(q = 1, 2, \ldots, n)$ time bin has a MPC (either ray or cluster) contribution to nth $(n \geq 2)$ time bin τ_n, denoted by $P_q^{(n)}$ can be calculated in three cases

$$P_q^{(n)} = \begin{cases} P_r, & q = 1 \\ P_c \cdot P_r, & 2 \leq q \leq n-1 \\ P_c, & q = n. \end{cases} \tag{16}$$

Proof of Lemma: See Appendix A.

[2]As for the cluster (first ray) arrival with significant path gain, the binomial approximation here seems to be sufficiently accurate, while it tends to be less accurate for the following ray arrival (with less significant path gain, especially for the CM1 channel model) because of much higher arrival rate [1].

It is very interesting to observe that, the probability that qth $(q = 1, 2, \ldots, n-1)$ time bin has a *ray* contribution to nth time bin can be simply calculated as the joint probability that a cluster arrives at qth time bin and this cluster results in a ray at nth time bin.

Using this lemma and enumerating all possible arrival patterns in nth time bin, the average path energy can be evaluated in Appendix B as

$$\begin{aligned}\boldsymbol{E}\left\{{A_1^{(\nu)}}^2\right\} &= \Omega_0 \\ \boldsymbol{E}\left\{{A_n^{(\nu)}}^2\right\} &= \Omega_0 P_c P_r \exp\left[-\frac{n\Delta\tau}{\gamma} + \frac{\Delta\tau}{\Gamma}\right]\frac{\rho^2(1-\rho^{n-2})}{1-\rho} \\ &\quad + \Omega_0 P_c \exp\left[-\frac{(n-1)\Delta\tau}{\Gamma}\right] \\ &\quad + \Omega_0 P_r \exp\left[-\frac{(n-1)\Delta\tau}{\gamma}\right]\end{aligned} \tag{17}$$

where $n \geq 2$ and $\rho = \exp\left(\frac{\Delta\tau}{\gamma} - \frac{\Delta\tau}{\Gamma}\right)$. Note that the user-specific superscript ν has been omitted in the final expression for notational simplicity. It should be pointed out that by defining $\bar{E}_c \triangleq \boldsymbol{E}\{\sum_{n=1}^{N}{A_n^{(\nu)}}^2\}$, we can now theoretically set

$$\Omega_0 = \frac{1}{\bar{E}_0} \triangleq \frac{1}{\bar{E}_c|_{\Omega_0=1}} \tag{18}$$

so as to make $\bar{E}_c = 1$ (normalized), instead of normalizing the total channel energy, which is defined as $\boldsymbol{E}\{\sum_{l=1}^{L}\sum_{k=1}^{K}|\alpha_{k,l}^{(\nu)}|^2\}$, for each realization as in [1]. By selecting the normalizing $\Omega_0 = \bar{E}_0^{-1}$ for each user and substituting (17) into (15), the channel-averaged output SINR is derived as

$$\begin{aligned}\text{SINR} &= \frac{E_w N_s R(0)^2 \Omega_0}{N_0 R(0) + E_w Q(0) T_f^{-1}(N_u - 1)} \\ &\quad \times \left[1 + P_c\frac{\exp\left(-\frac{\Delta\tau}{\Gamma}\right) - \exp\left(-\frac{L_p\Delta\tau}{\Gamma}\right)}{1-\exp\left(-\frac{\Delta\tau}{\Gamma}\right)}\right. \\ &\quad + P_r\frac{\exp\left(-\frac{\Delta\tau}{\gamma}\right) - \exp\left(-\frac{L_p\Delta\tau}{\gamma}\right)}{1-\exp\left(-\frac{\Delta\tau}{\gamma}\right)} + P_c P_r\frac{\rho^2\exp\left(\frac{\Delta\tau}{\Gamma}\right)}{1-\rho} \\ &\quad \times \left[\frac{\exp\left(-\frac{2\Delta\tau}{\gamma}\right) - \exp\left(-\frac{(L_p+1)\Delta\tau}{\gamma}\right)}{1-\exp\left(-\frac{\Delta\tau}{\gamma}\right)}\right. \\ &\quad \left.\left. - \frac{\exp\left(-\frac{2\Delta\tau}{\gamma}\right) - \rho^{L_p-1}\exp\left(-\frac{(L_p+1)\Delta\tau}{\gamma}\right)}{1-\exp\left(-\frac{\Delta\tau}{\Gamma}\right)}\right]\right].\end{aligned} \tag{19}$$

Note that the total channel energy is normalized to one for each user and the long-term lognormal shadowing has not been considered here, but it can easily be generalized to include it.

IV. Integration Interval Optimization for UWB-TR System

A direct application of the theoretical framework developed here is to determine the optimum integration interval for a UWB-TR system, so as to maximize average output SINR. This issue has been addressed by several previous papers [11]–[13]. However, all these papers only considered optimizing the integration interval in a single-user UWB-TR system. Besides, the optimum integration interval is found by simulation. In this section, we directly apply our theoretical framework, which will enable us to optimize the integration interval analytically, even in a multiuser scenario.

The transmitted signal from the νth user using biphase modulation is expressed by [12]

$$s^{(\nu)}(t) = \sum_{j=-\infty}^{+\infty} \sqrt{E_w}\, d_j^{(\nu)} \left[w_{tr}\left(t - jT_f - c_j^{(\nu)} T_c - \tau_0^{(\nu)}\right) + b_{\lfloor j/N_s \rfloor}^{(\nu)} w_{tr}\left(t - jT_f - c_j^{(\nu)} T_c - T_d^{(\nu)} - \tau_0^{(\nu)}\right)\right] \tag{20}$$

where the two transmitted pulses correspond to the reference and data pulses, respectively. $T_d^{(\nu)}$ is the user-specific delay between the reference and data pulses in each frame and is assumed to be larger than multipath delay spread T_m, so as to avoid the interference between the reference and data waveforms. In addition, the frame time T_f is assumed to be at least equal to $N_h^{(\nu)} T_c + T_m + T_w + T_d^{(\nu)}$ to ensure that there is no IFI. Note that the maximum TH shift $N_h^{(\nu)} T_c$ has been set accordingly, in order to keep the frame time T_f fixed for all users [12]. $d_j^{(\nu)}$ is a pseudorandom sequence to randomize the polarities of the transmitted pulses. All other parameters have been defined in Section II. To detect one of the νth user's transmitted symbols, a simple correlation receiver can be used to correlate the received signal with the one received $T_d^{(\nu)}$ seconds earlier and obtain the decision statistic by summing over N_s frames, i.e.,

$$Z^{(\nu)} = \sum_{j=0}^{N_s-1} \int_{jT_f + c_j^{(\nu)} T_c + \tau_0^{(\nu)} + T_d^{(\nu)}}^{jT_f + c_j^{(\nu)} T_c + \tau_0^{(\nu)} + T_d^{(\nu)} + T_{\text{corr}}} r(t) r\left(t - T_d^{(\nu)}\right) dt \tag{21}$$

where T_{corr} is assumed to be an integer multiple of the pulsewidth, denoted by $L_p T_w$. In order to clearly see the difference between single-user and multiuser UWB-TR systems when optimizing the integration interval, we separate our analysis into two cases.

A. Single User UWB-TR System

In a single-user UWB-TR system, the received signal in one symbol duration is written as

$$r(t) = \sum_{j=0}^{N_s-1} \sqrt{E_w}\, d_j^{(1)} \left[g^{(1)}\left(t - jT_f - c_j^{(1)} T_c - \tau_0^{(1)}\right) + b_{\lfloor j/N_s \rfloor}^{(1)} g^{(1)}\left(t - jT_f - c_j^{(1)} T_c - T_d^{(1)} - \tau_0^{(1)}\right)\right] + n(t) \tag{22}$$

where $g^{(1)}(t)$ has been defined before and $n(t)$ is AWGN with two-sided power spectral density of $N_o/2$. Using the correlation receiver mentioned earlier, the channel-averaged output SNR can be derived in Appendix III-A as a function of the integration interval via L_p

$$\text{SNR}(L_p) = \frac{N_s E_w^2 G^2(L_p)}{N_o E_w G(L_p) + N_o^2 W L_p T_w / 2} \tag{23}$$

where $G(L_p) \triangleq \sum_{i=1}^{L_p} \boldsymbol{E}\{A_i^{(1)^2}\}$ can be evaluated using (17), and W represents one-sided receiver bandwidth. As shown in Appendix C.1, the two terms in the denominator represent noise-times-signal and noise-times-noise terms, respectively. By substituting (17) into (23), we can theoretically determine the optimum integration interval via numerical search, given by

$$L_p^{\text{opt}} = \underset{L_p}{\text{argmax}} \{\text{SNR}(L_p)\} \tag{24}$$

which is a function of channel parameters, transmitted pulse energy, noise power spectral density, receiver bandwidth, and pulsewidth.

With noise only present, time bandwidth product given by $WT_{\text{corr}} = WL_pT_w$ largely affects the optimum integration interval (as long as the input SNR is high), because due to the multipath *resolvability condition*, most of the signal energy is captured as WT_{corr} reaches the number of multipath L present in the channel. Increasing WT_{corr} beyond this point will only accumulate more noise energy in the receiver as seen in the denominator of (23) and [15, eq. (12)]. However, as the input SNR decreases, the optimum integration interval via L_p decreases, because the channel gain coefficients $A_i^{(\nu)}$ in (4) could be zero if there is no arrival in the ith time bin, in which case noise energy is only accumulated.

B. Multiuser UWB-TR System

In the multiuser scenario, the received signal by the *desired* first user can be written as

$$\begin{aligned} r(t) = &\sum_{j=0}^{N_s-1} \sqrt{E_w} d_j^{(1)} \left[g^{(1)}\left(t - jT_f - c_j^{(1)} T_c - \tau_0^{(1)}\right) + b_{\lfloor j/N_s \rfloor}^{(1)} g^{(1)}\left(t - jT_f - c_j^{(1)} T_c - T_d^{(1)} - \tau_0^{(1)}\right)\right] + n(t) \\ &+ \sum_{\nu=2}^{N_u} \sum_{j=-\infty}^{+\infty} \sqrt{E_w} d_j^{(\nu)} \left[g^{(\nu)}\left(t - jT_f - c_j^{(\nu)} T_c - \tau_0^{(\nu)}\right) + b_{\lfloor j/N_s \rfloor}^{(\nu)} g^{(\nu)}\left(t - jT_f - c_j^{(\nu)} T_c - T_d^{(\nu)} - \tau_0^{(\nu)}\right)\right]. \end{aligned} \tag{25}$$

Besides AWGN as in single-user scenario, we have the MAI coming from other users, as long as their signals overlap with the first user's data or reference signals. Similar to the single-user case, the interference can be classified into three different types, such as MAI-times-signal, MAI-times-noise, and MAI-times-MAI.

As mentioned earlier, $T_d^{(\nu)}$ and $N_h^{(\nu)}$ are intentionally set to different values for different users. For instance, we may choose

$$T_d^{(\nu)} = T_m + (\nu - 1) T_w \;\text{ and }\; N_h^{(\nu)} = N_h^{(N_u)} - (\nu - 1) \tag{26}$$

TABLE I
AVERAGE TOTAL CHANNEL ENERGY $\bar{E}_0$ IN (18)

E_0	CM1	CM2
$N = 200$	13.3837	13.4105
N_{suff}	13.4297	13.6438
E_0	CM3	CM4
$N = 400$	33.2722	62.5121
N_{suff}	33.5808	67.5412

where we use the pulsewidth $T_w = T_c$. The main purpose for choosing different $T_d^{(\nu)}$ for different users is to misalign any other interferer's reference and data signals, so as to effectively reduce the MAI-times-MAI term. Specifically, the MAI-times-MAI can be further classified as two components. One is the total interference resulting from the correlation of the reference and data signals of the *same* interferer, termed it as self-MAI-times-MAI; the other is the total inteference resulting from the correlation of the reference and data signals of *different* interferers, termed it as cross-MAI-times-MAI. With the aforementioned signaling format, the contribution from self-MAI-times-MAI will be relatively small compared to cross-MAI-times-MAI, especially when the number of users is large. Consequently, we ignore the self-MAI-times-MAI term in the analysis for average output SINR, which will be validated by simulation.

Based on the earlier approximation, the channel-averaged output SINR is evaluated in Appendix III-B:

$$\begin{aligned}\text{SINR}(L_p) = N_s E_w^2 G^2(L_p) \Bigg\{ & N_o E_w G(L_p) \\ & + N_o^2 W L_p T_w/2 + 4(N_u-1)E_w^2 Q(0) T_f^{-1} G(L_p) \\ & + 2(N_u-1)E_w N_o L_p T_w T_f^{-1} + 4(N_u-1) \\ & \times (N_u-2) T_f^{-2} \Bigg[\int_0^{T_w} \int_{-y}^{T_w} R_w^2(x)\,dx\,dy \\ & + \int_0^{T_w} \int_{-T_w}^{T_w - y} R_w^2(x)\,dx\,dy \\ & + Q(0)(L_p-2)T_w \Bigg] \Bigg\}^{-1} \end{aligned} \tag{25}$$

where $R_w(\cdot)$ is defined as the autocorrelation function of the received pulse. Again, the optimum integration interval can be determined by (24) except using (27) as the objective function to be maximized. When both noise and MAI are present, and the MAI becomes dominant (i.e., when the input SNR is high), the MAI gets accumulated as T_{corr} (or L_p) increases as seen in the denominator of (27), which largely affects the optimum integration interval in the region of $WT_{\text{corr}} \le L$, unlike the case of only noise (i.e., a single user case) [15].

V. RESULTS

To first validate the theoretical framework developed in Section III, we choose $N = 200$ for CM1, CM2 and $N = 400$ for CM3, CM4 because the channel models CM1, CM2 and CM3, CM4 adopted in [1] have similar channel delay spreads, respectively. Note that $\Delta\tau$ is chosen to be 0.167 ns as suggested in [1], which is equal to the chip duration. With the long-term lognormal shadowing ignored, $\bar{E}_0$ in (18) is calculated for the channel models CM1, CM2, CM3, and CM4, as shown in Table I, where the total channel energy was also calculated using sufficiently large N, i.e., $N_{\text{suff}} \triangleq \lfloor 10(\Gamma+\gamma)/\Delta\tau \rfloor$ as suggested in [1]. It is seen that we can capture most of the signal energy when $N = 200$ for CM1, CM2 and $N = 400$ for CM3, CM4.

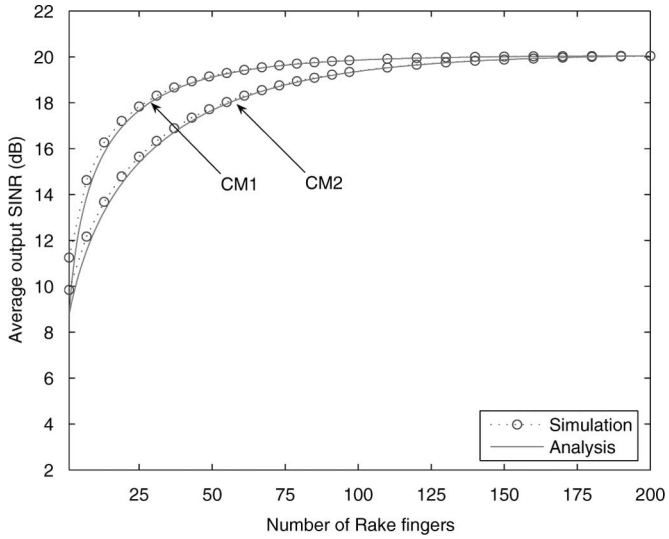

Fig. 1. Average output SINR versus number of Rake fingers for TH-BPPM UWB system, in CM1 and CM2 when $E_b/N_o = 20$ dB.

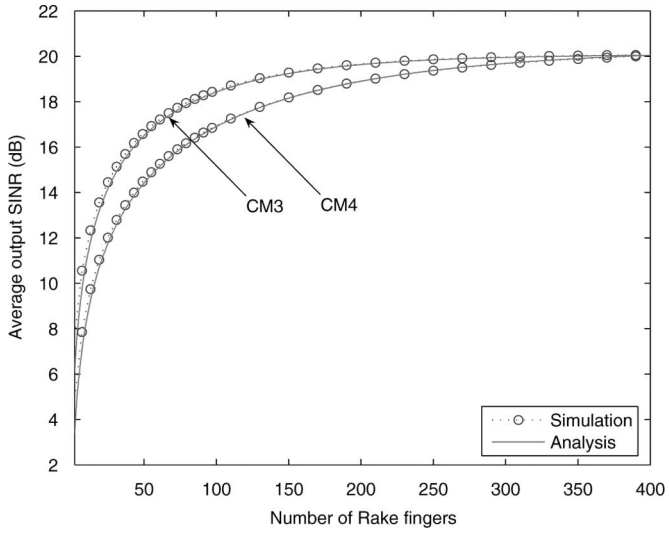

Fig. 2. Average output SINR versus number of Rake fingers for TH-BPPM UWB system, in CM3 and CM4 when $E_b/N_o = 20$ dB.

Next, we consider the Rake receiving system where $N_u = 20$ users experience the same channel condition and the received pulse is the second-order derivative Gaussian pulse with pulsewidth slightly less than $\Delta\tau$ to accomodate the time shift δ associated with BPPM. Also, the transmitted energy is normalized to $E_w = 1$. The frame time T_f is 1060 chips, which is around 180 ns and the pulse repetition is chosen as $N_s = 1$ without lost of generality. Figs. 1 and 2 show the average output SINR versus number of Rake fingers for the channel models CM1, CM2 and CM3, CM4, respectively, when $E_b/N_o = 20$ dB. We

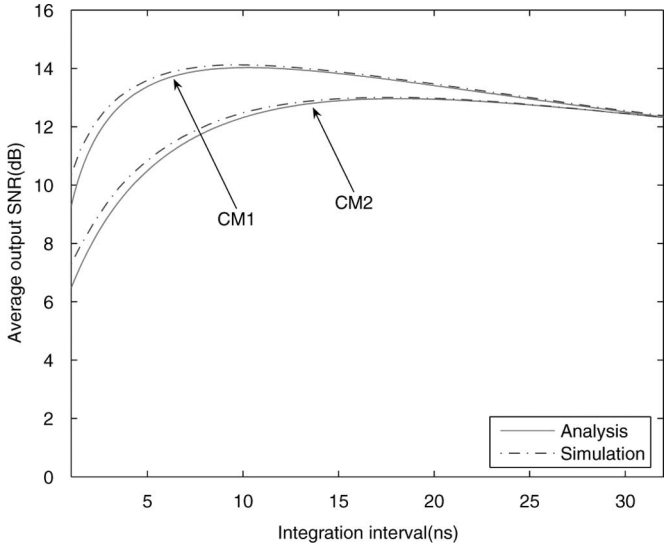

Fig. 3. Average output SNR versus integration interval for UWB-TR system, in CM1 and CM2 when $E_b/N_o = 20$ dB.

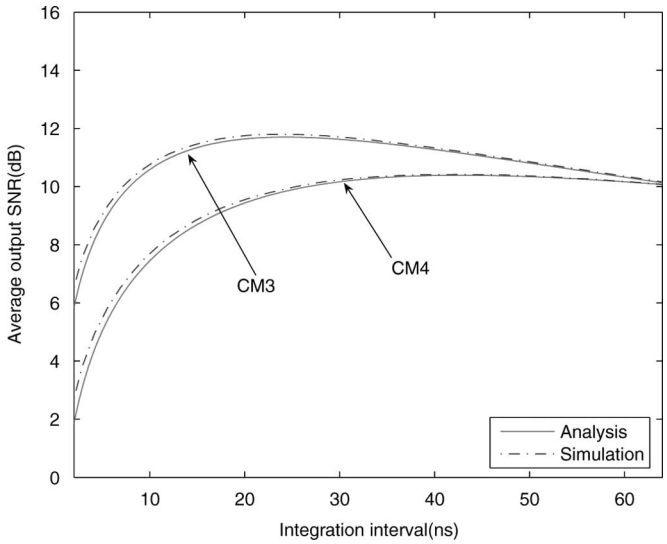

Fig. 4. Average output SNR versus integration interval for UWB-TR system, in CM3 and CM4 when $E_b/N_o = 20$ dB.

observe that our analysis matches well to the simulation results. The little discrepancies occurring for the small number of Rake fingers are mainly due to the 0.167 ns time bin, which is not small enough to well approximate the Poisson process by the binomial distribution. As observed in our simulations, in fact the discrepancies become less when smaller $\Delta\tau$ is adopted.

For the UWB-TR system, we choose the pulsewidth equal to the chip duration as we are using antipodal modulation and the frame time is chosen to be 1000 chips, which is around 167 ns. All other simulation parameters remain the same as in Rake receiving system. Figs. 3 and 4 show the average output SNR versus integration interval for a single-user UWB-TR system, from which we can see, for each type of channel model, there exists an optimum integration interval that maximizes the average output SNR. Specifically, in Figs. 3 and 4, $L_p^{\text{opt}}(T_w)$ are found to be 9.5, 17.5, 23.0, and 42.9 ns for CM1 to CM4, respectively. It is also to be noted that the average output SNRs in

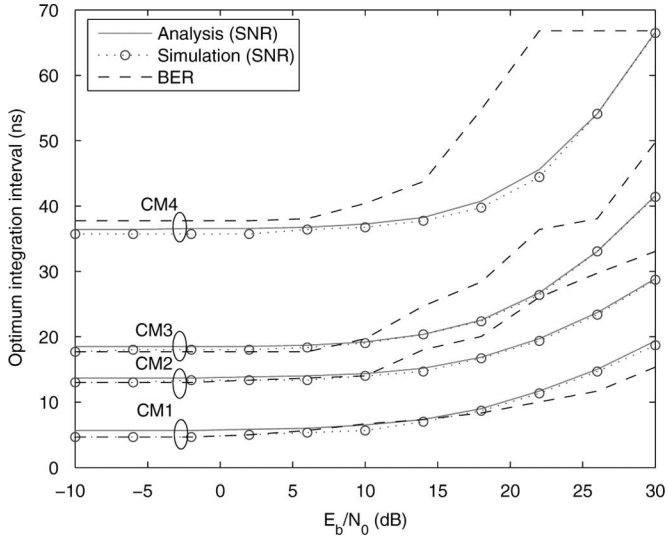

Fig. 5. Optimum integration interval versus E_b/N_o for UWB-TR system, in 4 different types of channel models CM1–CM4.

CM1 and CM2 converge to the same value, while the average output SNRs in CM3 and CM4 converge to another value. This can be explained from (23) that as L_p increases and finally approaches N, $G(L_p) \to 1$ and the convergence point, which the average output SNR will reach depends on the choice of N.

Fig. 5 shows how the optimum integration interval depends upon input SNR for CM1–CM4. It is observed that when the input SNR increases, the optimum integration interval also increases. We can also find that, when the input SNR is very small, there exists a lower bound on the optimum integration interval for each type of channel model, which is found to be approximately 4.7, 13.0, 18.0, and 35.7 ns for CM1–CM4, respectively. This is an important system design parameter in the sense that in order to ensure a maximum average output SNR, the integration interval should be at least equal to this value. It should also be pointed out that the integration interval determined by maximizing average output SNR may not be optimum in terms of minimizing average BER. To check the goodness of the optimized integration time, Fig. 5 also includes the integration intervals corresponding to minimum average BER for each input SNR. It is obvious that the two criterions yield similar results for low and medium SNRs, while exhibiting some differences for high SNR.

Fig. 6 show the average BER performance for a single-user UWB-TR system for CM2 and CM4, respectively. Here, we compare the performance of the scheme that *adaptively* chooses the optimum integration interval depending on input SNR, with the one using the lower bound for all input SNR values. As a reference, we also include the curve corresponding to minimum average BER. It is easy to find that the adaptive scheme achieves almost the same performance as the one minimizing average BER. Moreover, it outperforms the one using the lower bound as the input SNR increases.

Fig. 7 provides the validation for the approximation made in (28) (i.e., ignoring the self-MAI-times-MAI term) when analyzing the channel-averaged output SINR for the multiuser

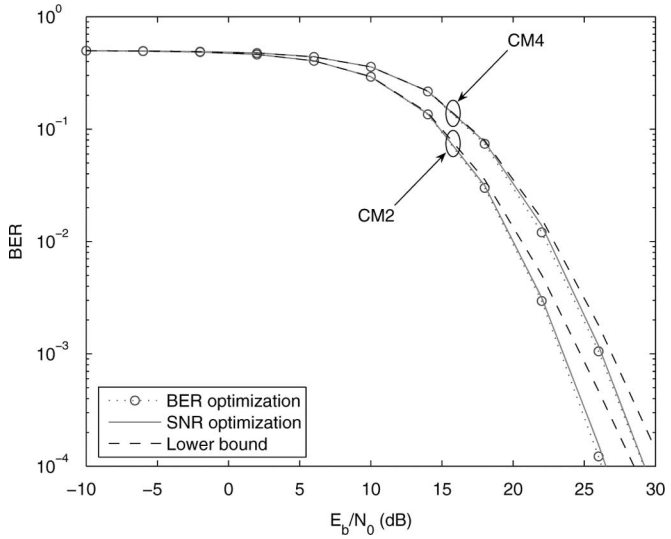

Fig. 6. BER performance versus E_b/N_o with adaptively selected integration intervals for UWB-TR system, in CM2 and CM4.

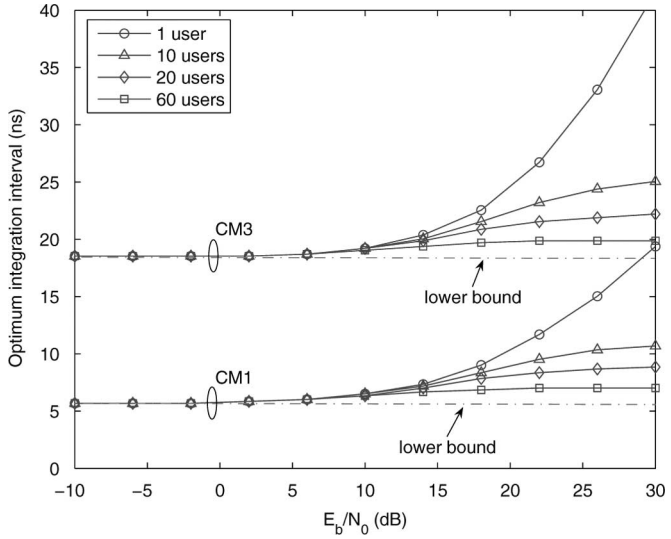

Fig. 8. Optimum integration interval versus E_b/N_o for UWB-TR system, in CM1 and CM3 under the multiuser scenario.

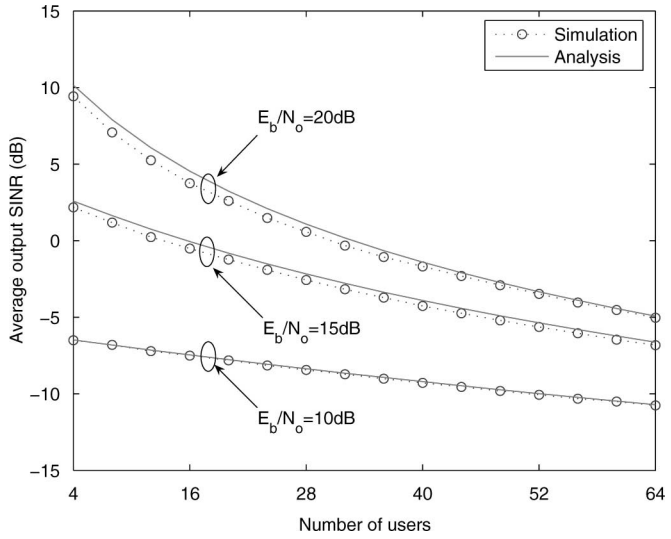

Fig. 7. Average output SINR versus number of users for UWB-TR system, with different E_b/N_o in CM1.

UWB-TR system. As an example, the average output SINR for CM1 is presented for different input SNR values. Note that we have used the integration interval equal to channel delay spread T_m, which corresponds to the worst case for our approximation. In fact, as the integration interval decreases, the approximation becomes more accurate. As we can see, the approximation approaches the simulation results as the number of users increases and the discrepancies become smaller as the input SNR decreases. Even for the high SNR (e.g., 20 dB), which seems to be an operating SNR range with TR systems, our approximation is still within acceptable range from the simulation results.

Fig. 8 shows the theoretical optimum integration interval for the multiuser UWB-TR system for CM1 and CM3. It is found that, as far as the MAI is concerned, the optimum integration interval will be decreased compared to a single-user UWB-TR system. Especially, when the number of users is large, the optimum integration interval approaches the lower bound that has been observed in the single-user system for very low input SNR. This result, combined with Fig. 6, suggests that in the dense multiuser UWB-TR system, a good choice for the integration interval is to simply use the lower bound, which somehow reduces receiver complexity (shorter and fixed integration time) without causing too much performance loss.

VI. Conclusion

We have derived a theoretical closed-form expression for the *channel-averaged* output SINR under IEEE 802.15.3a channel model, assuming the Rake receivers in a multiuser scenario. The theoretical framework developed here can be used to evaluate the channel-averaged output SINR as a useful performance measure for the UWB Rake receiving system under different types of indoor wireless channel models. This framework also enables us to theoretically determine the optimum integration interval, which yields the maximum average output SNR for a single-user UWB-TR system. We investigated the BER performance, using the optimum integration interval and observed that using the lower bound as the integration interval for all input SNRs causes some performance loss. We extended the analysis to the multiuser UWB-TR system and demonstrated that the optimum integration interval is different from that for the single-user system. We also found that, in the multiuser scenario, using the lower bound as the integration interval is a good choice, especially in the dense multiuser system.

Appendix I

Proof of Lemma

Case 1: for $q = 1$, we always have the first cluster ($l = 0$) arrived in the first time bin. The probability that this cluster has

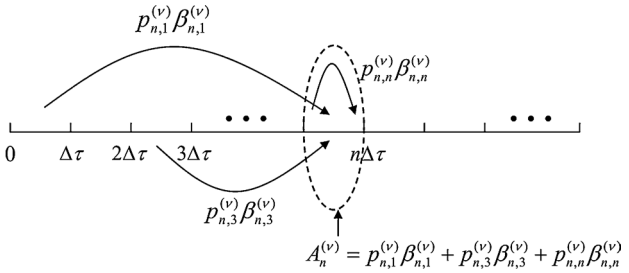

Fig. 9. One possible channel realization for the nth time bin.

a ray contribution to nth time bin is calculated to be

$$P_1^{(n)} = \sum_{k=1}^{n-1} Pr[\tau_{k,\,0} = (n-1)\Delta\tau] = \sum_{k=1}^{n-1} P_r \binom{n-2}{k-1} P_r^{k-1}(1-P_r)^{n-k-1} = P_r. \quad (28)$$

Case 2: for $2 \le q \le n-1$, the probability that qth time bin has a ray contribution to nth time bin can be derived in a similar way as

$$\begin{aligned} P_q^{(n)} &= \sum_{l=1}^{q-1} Pr[T_l = (q-1)\Delta\tau] \sum_{k=1}^{n-q} Pr[\tau_{k,\,l} = (n-q)\Delta\tau] \\ &= \sum_{l=1}^{q-1} Pr[T_l = (q-1)\Delta\tau] \sum_{k=1}^{n-q} P_r \binom{n-q-1}{k-1} \\ &\quad \times P_r^{k-1}(1-P_r)^{n-q-k} \\ &= P_r \sum_{l=1}^{q-1} Pr[T_l = (q-1)\Delta\tau] \\ &= P_r \sum_{l=1}^{q-1} P_c \binom{q-2}{l-1} P_c^{l-1}(1-P_c)^{q-l-1} \\ &= P_c P_r. \end{aligned} \quad (29)$$

Case 3: for $q = n$, the probability $P_q^{(n)}$ is equivalent to the probability of a cluster arrival, which is P_c.

Appendix II
Evaluation of Average Path Energy

Consider the first cluster in the first time bin ($\tau_1 = 0$) that occurs with probability one, then we have

$$\boldsymbol{E}\left\{A_1^{(\nu)^2}\right\} = \Omega_0. \quad (30)$$

For the time bins other than the first one, due to our mathematical modeling, the $(n-1)$ preceding time bins may contribute ray components to nth time bin. In addition, nth time bin may have a cluster contribution to itself.

Fig. 9 illustrates one possible channel realization for nth time bin, in which $\beta_{n,q}^{(\nu)}$ represents the MPC in nth time bin contributed by qth time bin, along with $p_{n,q}^{(\nu)}$ equiprobably taking on the value of ± 1. We can see that in Fig. 9, the first and third time bins have ray contributions to nth time bin and nth time bin has a cluster contribution to itself. Recall that, in the discrete-time channel model of (4), the combined channel coefficient $A_n^{(\nu)}$ denotes the sum of the channel coefficients of all the MPCs in nth time bin and this accounts for any possible *cluster overlapping*, which is an important channel characteristic of IEEE 802.15.3a channel model, especially for the NLOS channel models CM2, CM3, and CM4. Consequently, by defining

$$U_{n,q}^{(\nu)} = \begin{cases} 1, & \text{if the } q\text{th time bin has a MPC contribution} \\ & \text{to the } n\text{th time bin} \\ 0, & \text{otherwise} \end{cases} \quad (31)$$

the combined channel coefficient $A_n^{(\nu)}$ can be written as

$$A_n^{(\nu)} = \sum_{q=1}^{n} p_{n,q}^{(\nu)}\, \beta_{n,q}^{(\nu)}\, U_{n,q}^{(\nu)}. \quad (32)$$

When taking the expectation for $A_n^{(\nu)^2}$, we can use the similar relation as given in (13) and all the crossterms will disappear, leading to

$$\begin{aligned} \boldsymbol{E}\{A_n^{(\nu)^2}\} &= \sum_{q=1}^{n} \boldsymbol{E}\{p_{n,q}^{(\nu)^2}\beta_{n,q}^{(\nu)^2}U_{n,q}^{(\nu)^2}\} \qquad (n \ge 2) \\ &= \sum_{q=1}^{n} \boldsymbol{E}\{\beta_{n,q}^{(\nu)^2}U_{n,q}^{(\nu)^2}|U_{n,q}^{(\nu)} = 1\}Pr[U_{n,q}^{(\nu)} = 1] \\ &= \sum_{q=1}^{n} \boldsymbol{E}\{\beta_{n,q}^{(\nu)^2}\}Pr[U_{n,q}^{(\nu)} = 1] \end{aligned} \quad (33)$$

where the probability of having $U_{n,q}^{(\nu)} = 1$ is simply $P_q^{(n)}$, which is given by the lemma in (16). Furthermore, according to the IEEE 802.15.3a channel model [1], we have

$$\boldsymbol{E}\{\beta_{n,q}^{(\nu)^2}\} = \Omega_0 \exp\left[-\frac{(q-1)\Delta\tau}{\Gamma}\right] \exp\left[-\frac{(n-q)\Delta\tau}{\gamma}\right] \quad (34)$$

Substituting (16) and (34) into (33), then combining with (30), we will finally obtain (17).

Appendix III

A. Average SNR for Single-User UWB-TR System

The decision statistic of a single-user UWB-TR system, defined by (20), can be rewritten as

$$Z^{(1)} = \xi + n_1 + n_2 \quad (35)$$

where the three terms of right-hand side represent desired signal, noise-times-signal, noise-times-noise, respectively. The desired signal energy is easily evaluated as

$$|\boldsymbol{E}\{\xi\}|^2 = N_s^2 E_w^2 G^2(L_p). \quad (36)$$

It is easy to show that n_1 and n_2 are zero-mean and independent of each other. Furthermore, the variance of n_1 is easily

evaluated to be

$$\sigma_{n_1}^2 = N_s E_w N_o G(L_p). \tag{37}$$

As for the noise-times-noise term, the autocorrelation function $r_n(\tau)$ for the front-end filtered noise can be expressed as

$$r_n(\tau) = N_o W \mathrm{sinc}(2W\tau). \tag{38}$$

According to [16], the variance for the noise-times-noise term can be calculated as

$$\sigma_{n_2}^2 = 2N_s \int_0^{T_{\text{corr}}} (T_{\text{corr}} - \tau) r_n^2(\tau)\, d\tau. \tag{39}$$

Substituting (38) into (39), we obtain

$$\begin{aligned}\sigma_{n_2}^2 &= 2N_s N_o^2 W^2 \int_0^{T_{\text{corr}}} (T_{\text{corr}} - \tau)\, \mathrm{sinc}^2(2W\tau)\, d\tau \\ &= N_s N_o^2 W T_{\text{corr}} \left[\int_0^{2WT_{\text{corr}}} \mathrm{sinc}^2(t)\, dt \right. \\ &\quad \left. + \frac{1}{2WT_{\text{corr}}} \int_0^{2WT_{\text{corr}}} t\, \mathrm{sinc}^2(t)\, dt \right].\end{aligned} \tag{40}$$

Using the sine integral and cosine integral special functions, the first and second terms inside brackets of (40) can be evaluated as ($x \triangleq 2WT_{\text{corr}}$)

$$\int_0^x \mathrm{sinc}^2(t)\, dt = \frac{1}{2} - x\,\mathrm{sinc}^2(x) + \frac{1}{\pi}\,\mathrm{si}(2\pi x) \tag{41}$$

$$\frac{1}{x}\int_0^x t\,\mathrm{sinc}^2(t)\, dt = \frac{1}{2\pi^2 x}\left[\ln(\pi x) + \mathcal{C} - \mathrm{ci}(2\pi x)\right] \tag{42}$$

where the special functions are defined by $\mathrm{si}(y) = -\int_y^\infty \frac{\sin t}{t}\, dt$ and $\mathrm{ci}(y) = -\int_y^\infty \frac{\cos t}{t}\, dt$, and $\mathcal{C}$ is Euler's constant. Typically, WT_{corr} (i.e., the number of MPCs being captured) is very large for UWB channels in which case (41) can be well approxiamted to 1/2 while (42) is relatively ignored, resulting in

$$\sigma_{n_2}^2 \approx \frac{1}{2} N_s N_o^2 W T_{\text{corr}}. \tag{43}$$

Combining (36), (37) and (43), we will finally derive (23).

B. Average SINR for Multiuser UWB-TR System

The decision statistic can now be rewritten as

$$Z^{(1)} = \xi + n_1 + n_2 + n_3 + n_4 + n_5 \tag{44}$$

where the three extra terms of right-hand side represent MAI-times-signal, MAI-times-noise and MAI-times-MAI, respectively. We refer to the [12, eq. (21)], by applying our framework, and will easily derive

$$\sigma_{n_3}^2 = 4(N_u - 1) N_s E_w^2 Q(0) T_f^{-1} G(L_p) \tag{45}$$

$$\sigma_{n_4}^2 = 2(N_u - 1) N_s E_w N_o R_w(0) L_p T_w T_f^{-1} \tag{46}$$

$$\begin{aligned}\sigma_{n_5}^2 &\approx 4(N_u - 1)(N_u - 2) N_s T_f^{-2} \left[\int_0^{T_w} \int_{-y}^{T_w} R_w^2(x)\, dx\, dy \right. \\ &\quad \left. + \int_0^{T_w} \int_{-T_w}^{T_w - y} R_w^2(x)\, dx\, dy + Q(0)(L_p - 2) T_w \right].\end{aligned} \tag{47}$$

Note that (47) has ignored the self-MAI-times-MAI term. Finally, combining (36), (37), (43) and (45)–(47), the channel-averaged SINR in (27) follows.

REFERENCES

[1] J. Forester, "Channel Modeling Sub-committee Report Final," Tech. Rep. IEEE P802.15-02/368r5-SG3a, Nov. 2002.

[2] M. Z. Win and R. A. Scholtz, "Impulse radio: How it works," *IEEE Commun. Lett.*, vol. 2, no. 2, pp. 36–38, Feb. 1998.

[3] M. Z. Win and R. A. Scholtz, "Ultra-wide bandwidth time-hopping spread-spectrum impulse radio for wireless multiple-access communications," *IEEE Trans. Commun.*, vol. 48, no. 4, pp. 679–691, Apr. 2000.

[4] B. Hu and N. C. Beaulieu, "Accurate evaluation of multiple-access performance in TH-PPM and TH-BPSK UWB systems," *IEEE Trans. Commun.*, vol. 52, no. 10, pp. 1758–1766, Oct. 2004.

[5] M. Z. Win and R. A. Scholtz, "On the robustness of ultra-wide bandwidth signals in dense multipath environments," *IEEE Commun. Lett.*, vol. 2, no. 2, pp. 51–53, Feb. 1998.

[6] M. Z. Win and R. A. Scholtz, "On the energy capture of ultra-wide bandwidth signals in dense multipath environments," *IEEE Commun. Lett.*, vol. 2, no. 9, pp. 245–247, Sep. 1998.

[7] A. Rajeswaran, V. S. Somayazulu, and J. R. Foerster, "Rake performance for a pulse based UWB system in a realistic UWB indoor channel," in *Proc. IEEE Int. Conf. Commun.*, May 2003, vol. 4, pp. 2879–2883.

[8] M. A. Rahman, S. Sasaki, J. Zhou, S. Muramatsu, and H. Kikuchi, "Performance evaluation of Rake reception of ultra wideband signals over multipath channels from energy capture perspective," in *Proc. Joint UWBST IWUWBS*, May 2004, pp. 231–235.

[9] Y. Ishiyama and T. Ohtsuki, "Performance comparison of UWB-IR using Rake receivers in UWB channel models," in *Proc. Joint UWBST IWUWBS*, May 2004, pp. 226–230.

[10] R. T. Hoctor and H. W. Tomlinson, "An overview of delay-hopped transmitted-reference RF communications," G. E. Res. Develop. Center,Tech. Rep. 2001CRD198, Jan. 2002.

[11] S. Franz and U. Mitra, "Integration interval optimization and performance analysis for UWB transmitted reference systems," in *Proc. Joint UWBST IWUWBS*, May 2004, pp. 26–30.

[12] Y.-L. Chao and R. A. Scholtz, "Multiple access performance of ultra-wideband transmitted reference systems in multipath environments," in *Proc. IEEE WCNC*, Mar. 2004, vol. 3, pp. 1788–1793.

[13] F. Tufvesson and A. F. Molisch, "Ultra-wideband communication using hybrid matched filter correlation receivers," in *Proc. IEEE VTC Spring '04*, vol. 3, pp. 1290–1294.

[14] G. L. Stüber, *Principles of Mobile Communication*, 2nd ed. Norwell, MA: Kluwer, 2001.

[15] T. Q. S. Quek and M. Z. Win, "Analysis of UWB transmitted-reference communication systems in dense multipath channel," *IEEE J. Sel. Areas Commun.*, vol. 23, no. 9, pp. 1863–1874, Sep. 2005.

[16] A. Papoulis, *Probability, Random Variables, and Stochastic Processes*, 2nd ed. New York: McGraw-Hill, 1984.

Tao Jia (S'05) received the B.Eng. and M.A.Sc. degrees in electrical engineering from the University of Science and Technology of China (USTC), Hefei, China, and Simon Fraser University, Burnaby, Canada, in 2003 and 2006, respectively. He is currently working toward the Ph.D. degree in the Mobile and Portable Radio Research Group (MPRG) at Virginia Polytechnic Institute and State University (Virginia Tech), Blacksburg.

He is currently with the Bradley Department of Electrical and Computer Engineering, Virginia Polytechnic Institute and State University (Virginia Tech), Blacksburg, VA. His current research interests include position location in wireless sensor networks, physical layer design, and performance analysis for ultrawideband (UWB) communication systems, software defined radio (SDR), and cognitive radio system.

Dong In Kim (S'89–M'91–SM'02) received the B.S. and M.S. degrees in electronics engineering from Seoul National University, Seoul, Korea, in 1980 and 1984, respectively, and the second M.S. and Ph.D. degrees in electrical engineering from the University of Southern California (USC), Los Angeles, in 1987 and 1990, respectively.

From 1984 to 1985, he was a Researcher with Korea Telecom Research Center, Seoul. From 1986 to 1988, he was a Korean Government Graduate Fellow in the Department of Electrical Engineering, USC. From 1991 to 2002, he was with the University of Seoul, Seoul, leading the Wireless Communications Research Group. From 2002 to 2007, he was a tenured Full Professor in the School of Engineering Science, Simon Fraser University, Burnaby, BC, Canada. From 1999 to 2000, he was a Visiting Professor at the University of Victoria, Victoria, BC. Since 2007, he has been with Sungkyunkwan University, Suwon, Korea, where he is currently a Professor and University Fellow in the School of Information and Communication Engineering. Since 1988, he is engaged in the research activities in the areas of cellular radio networks and spread-spectrum systems. His current research interests include wideband, broadband, and ultrawideband (UWB) code division multiple access (CDMA) for high-data-rate wireless multimedia, signal design and diversity techniques for CDMA/UWB, and cross-layer design for CDMA/UWB systems.

Dr. Kim was the Editor of the IEEE JOURNAL ON SELECTED AREAS IN COMMUNICATIONS: WIRELESS COMMUNICATIONS SERIES and also a Division Editor of the *Journal of Communications and Networks*. He is currently the Editor of the Spread Spectrum Transmission and Access for the IEEE TRANSACTIONS ON COMMUNICATIONS and the IEEE TRANSACTIONS ON WIRELESS COMMUNICATIONS.